Neurosci. Bull. June, 2016, 32(3):246–252
DOI 10.1007/s12264-016-0029-6

www.neurosci.cn
www.springer.com/12264

REPORT

# Biophotons Contribute to Retinal Dark Noise

**Zehua Li[1,2] · Jiapei Dai[1,2]**

Received: 26 October 2015 / Accepted: 6 March 2016 / Published online: 8 April 2016


**Abstract** The discovery of dark noise in retinal photoreceptors resulted in a long-lasting controversy over its origin and the underlying mechanisms. Here, we used a novel ultra-weak biophoton imaging system (UBIS) to detect biophotonic activity (emission) under dark conditions in rat and bullfrog (*Rana catesbeiana*) retinas *in vitro*. We found a significant temperature-dependent increase in biophotonic activity that was completely blocked either by removing intracellular and extracellular $Ca^{2+}$ together or inhibiting phosphodiesterase 6. These findings suggest that the photon-like component of discrete dark noise may not be caused by a direct contribution of the thermal activation of rhodopsin, but rather by an indirect thermal induction of biophotonic activity, which then activates the retinal chromophore of rhodopsin. Therefore, this study suggests a possible solution regarding the thermal activation energy barrier for discrete dark noise, which has been debated for almost half a century.

**Keywords** Biophoton · Rat and bullfrog retinas · Retinal dark noise · Phosphodiesterase 6 · $Ca^{2+}$ · Biophoton imaging

## Introduction

The discovery of dark noise in the membrane currents of retinal photoreceptors improved our understanding of the fundamental limit of visual sensitivity. However, its origin and underlying mechanisms remain unclear. There are two components of dark noise in rods: discrete photon-like events caused by the spontaneous activation of rhodopsin and continuous current fluctuations caused by the spontaneous activation of phosphodiesterase (PDE) [1, 2]. The discrete components of noise are indistinguishable from those produced by real photon-induced photoisomerization with respect to shape and duration. Nevertheless, several studies have suggested mechanisms for the thermal activation of rhodopsin: isomerization occurring in a rhodopsin population in which the chromophore is deprotonated [3], simultaneous hydrolysis and thermal isomerization of the 11-cis retinal protonated Schiff base chromophore covalently linked to the opsin core [4], a change in the hydrogen-bonding network near the active site [5], fluctuations in the protein structure [6], and quantum chemical models [7, 8]. However, such studies have not yet provided a reasonable interpretation or experimental evidence to resolve the key problem of the thermal activation energy barrier. The calculated activation energy of the thermal process in toad rhodopsin is about 22 kcal/mol, which is significantly less than the energy necessary for activation by single photon (about 40–50 kcal/mol). Some studies question the validity of the measured activation barrier because it assumes Boltzmann statistics [9, 10], so the Hinshelwood distribution should be used instead of the Boltzmann distribution [10]. However, a computational study suggested that the barrier is correct but the stored energy is not [11]. In addition, these mechanistic models do not explicitly address the experimentally-observed Barlow correlation

✉ Jiapei Dai
jdai@mail.scuec.edu.cn

[1] Wuhan Institute for Neuroscience and Neuroengineering, South Central University for Nationalities, Wuhan 430074, China

[2] Department of Neurobiology, College of Life Sciences, South Central University for Nationalities, Wuhan 430074, China

[12, 13], which establishes a relationship between the pigment thermal activation kinetic constant (k) and the maximum absorption wavelength. This provides a link between thermal and photochemical activation, for which a thorough mechanism must offer an explanation.

Biophotons, or ultra-weak photon emissions (UPE), are extremely weak photon beams that are characteristically similar to the Poisson coherent field, radiated spontaneously in normal or pathological conditions in virtually all organisms, including humans [14]. It has been suggested that biophotons, being a coherent electromagnetic field inside of cells, which are emitted by the excited atom's outer electrons when they return to the ground state, may be a basis for cell-to-cell communication [15–17] and play an important role in the processing of neural information through a mechanism of biophotonic transmission [18–20]. Here, we provide experimental evidence, for the first time, that temperature-dependent biophotonic activity (emission) may contribute to retinal dark noise.

## Materials and Methods

### Rat and Toad Retina Preparations

Retinas were obtained from male Wistar rats (2–3 months old) and large tropical toads (bullfrogs, *Rana catesbeiana*, 275–360 g). This study was carried out under strict accordance with the recommendations in the Guide for the Care and Use of Laboratory Animals of the National Institutes of Health. Rats were housed under standard conditions (12-h light/dark cycle; 20–23 °C; 40%–60% humidity) with food and water *ad libitum*. Bullfrogs were obtained from a commercial supplier and kept in a tank in which they were permitted free access to a pool of running water, a dry platform, and food. Both rats and bullfrogs were darkly adapted overnight before each experiment. The protocols were approved by the Committee on the Ethics of Animal Experiments of South-Central University for Nationalities.

Bullfrogs were pithed and rats were decapitated. One eye was quickly removed in dim red light and placed in ice-cold (4 °C) artificial cerebral spinal fluid (ACSF) (rat eye) or Ringer's solution (bullfrog eye) for about 5 min. The ACSF contained (in mmol/L) 125 NaCl, 2.5 KCl, 2 $CaCl_2$, 1 $MgCl_2$, 1.25 $NaH_2PO_4$, 26 $NaHCO_3$, and 20 D-glucose; pH 7.4. The Ringer's solution contained (in mmol/L) 111 NaCl, 1.6 $MgCl_2$, 2.5 KCl, 1.0 $CaCl_2$, 10 D-glucose, 3 HEPES, pH 7.8; they were continuously bubbled with 95% $O_2$ and 5% $CO_2$. The whole retina was carefully isolated and incubated in either ACSF or Ringer's solution at room temperature (23 °C) for a minimum of 1 h before imaging.

### Perfusion Temperature Maintenance and Change

The temperature of the medium in the perfusion chamber was maintained with an electrical heater combined with a calibrated thermistor attached to the suction electrode and positioned within 0–5 mm of its tip. A temperature change reached its final value in about 2 min.

### *In vitro* Biophoton Imaging System and Imaging Processes

Retinas were submerged in a perfusion bath of ACSF or Ringer's solution (200 mL) that was contained in a glass bottle. A mixture of 95% $O_2$ and 5% $CO_2$ was constantly supplied with a membrane oxygenator in the solution during the perfusion period. The perfusion was maintained by input and output micropumps (5 mL/min) outside the dark box.

The *in vitro* ultra-weak biophoton imaging system (UBIS) and imaging processes are described in our recent study [19]. The other setup parameters during imaging were photon detection model 3, 16 binning, and 1200 gain. The specific steps for biophoton detection and imaging were as follows: (1) the retinas were transferred to a chamber and kept in complete darkness for about 30 min before imaging; (2) a regular image of each whole retina was taken under the normal CCD mode before and after the imaging processes in order to locate its position in the imaging field of view (Fig. 1A, H); and (3) real-time imaging by automatic image capture every 1 min.

### Drug Treatments

A phosphodiesterase 6 (PDE6) inhibitor (Zaprinast, 100 nmol/L, Sigma, St. Louis, MO), BAPTA-AM (10 μmol/L, Molecular Probes, Eugene, OR), and EGTA (0.5 mmol/L, Amresco, Solon, OH) were initially dissolved in DMSO and then diluted to their final concentrations in ACSF or Ringer's solution.

### Image Processing and Data Analysis

Image processing and data analysis were as described in our recent study [19]. The specific processes were as follows: (1) all original images were processed with a program running on the MATLAB platform. This method provided two kinds of images: processed biophoton gray images and the biophoton number images; (2) the processed images were analyzed for the average gray value (AGV) in the region of interest (ROI, here whole retina area) using image analysis software (HCImage Version 1.1.3.1, Hamamatsu Photonics K. K., Hamamatsu, Japan)

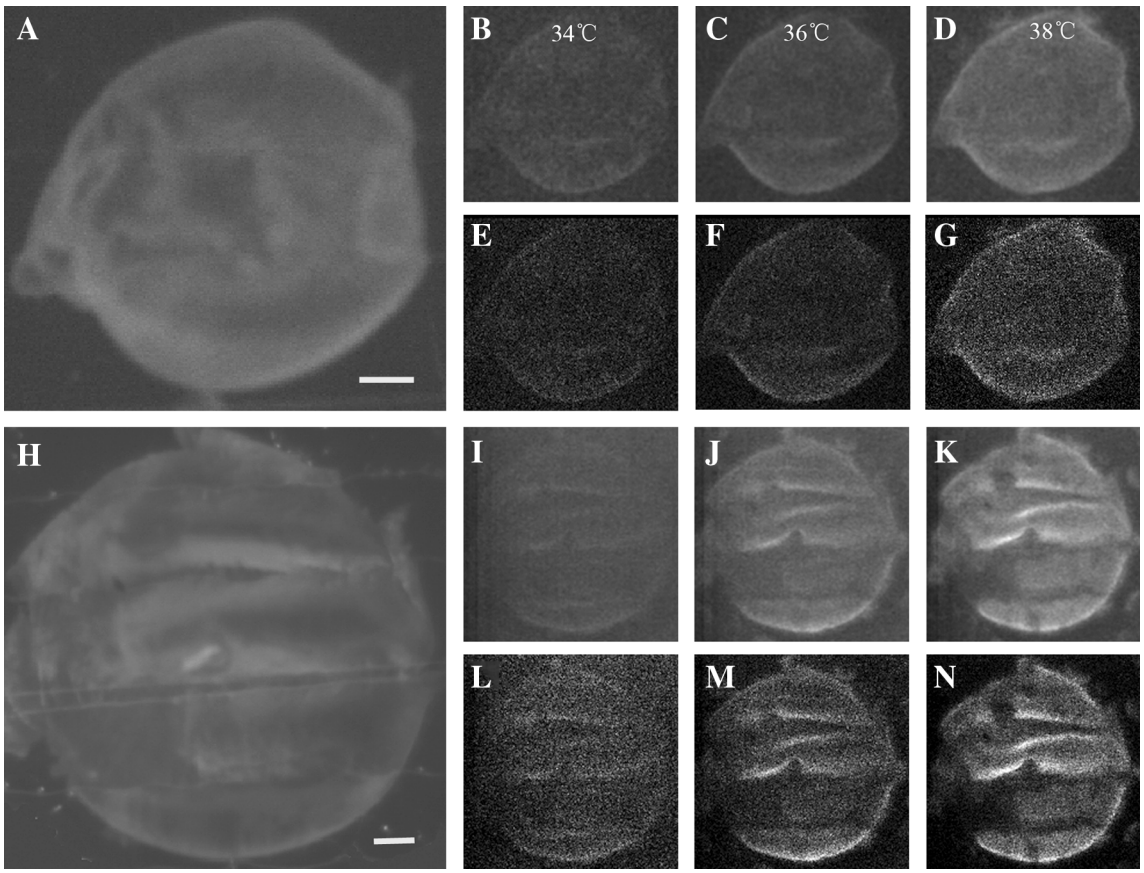


**Fig. 1** Imaging biophotonic activity in rat and bullfrog retinas. **A** Representative regular image of a whole rat retina. **B–G** Representative biophoton gray images (**B**-**D**) and corresponding biophoton number images (**E–G**) at 34, 36, and 38 °C. **H** Representative regular image of a whole bullfrog retina. **I–N** Representative biophoton gray images (**I–K**) and corresponding biophoton number images (**L–N**) at 34, 36, and 38 °C. Each image in **B–G** and **I–N** was obtained from the merger of 90 continuously-processed original gray images or biophoton number images (1-min imaging time for each original image). Temperatures (34, 36 and 38 °C) indicated in **B**, **C**, and **D** are the same for **E**, **I**, and **L**; **F**, **J**, and **M**; and **G**, **K**, and **N**, respectively. *Scale bars* 1 mm for **A** and **H**.

[*note: The gray value extends from 0 pixels (minimum) to 65025 pixels (maximum, 255 × 255). A lower value (fewer biophotons) means darker and a higher value (more biophotons) means brighter. Therefore, the gray value represents the biophoton signal strength*]. The relative gray value (RGV) was calculated as RGV = AGV (ROI) − AGV (Non-ROI), where AGV (Non-ROI) is the AGV in the region of non-interest of an image (considered as background biophoton emission based on our previous study [19]); and (3) the biophoton number of images (BNIs) in the ROI were obtained from the biophoton number images with the same software.

### Statistical Analysis

Statistical analyses were performed using Microsoft Excel. A two-tailed paired *t*-test was used to compare the effects of temperature at different time points. A two-tailed Student's *t*-test was used to compare the effects of the control and treated groups at different time points.

## Results and Discussion

### Temperature-Dependent Biophotonic Activity in Rat and Bullfrog Retinas

The biophotonic activity in rat and bullfrog retinas was detected and imaged spatiotemporally across a range of temperatures (34, 36, and 38 °C) in darkness. We found that both retinas emitted biophotons in the absence of external light excitation, based on analysis of the RGVs (Fig. 1B–D, I–K) and BNIs (Fig. 1E–G, L–N). A temperature-dependent increase in biophotonic activity was found in both rat (Figs. 1E–G, 2A–G) and bullfrog (Figs. 1L–N, 2H–N) retinas.

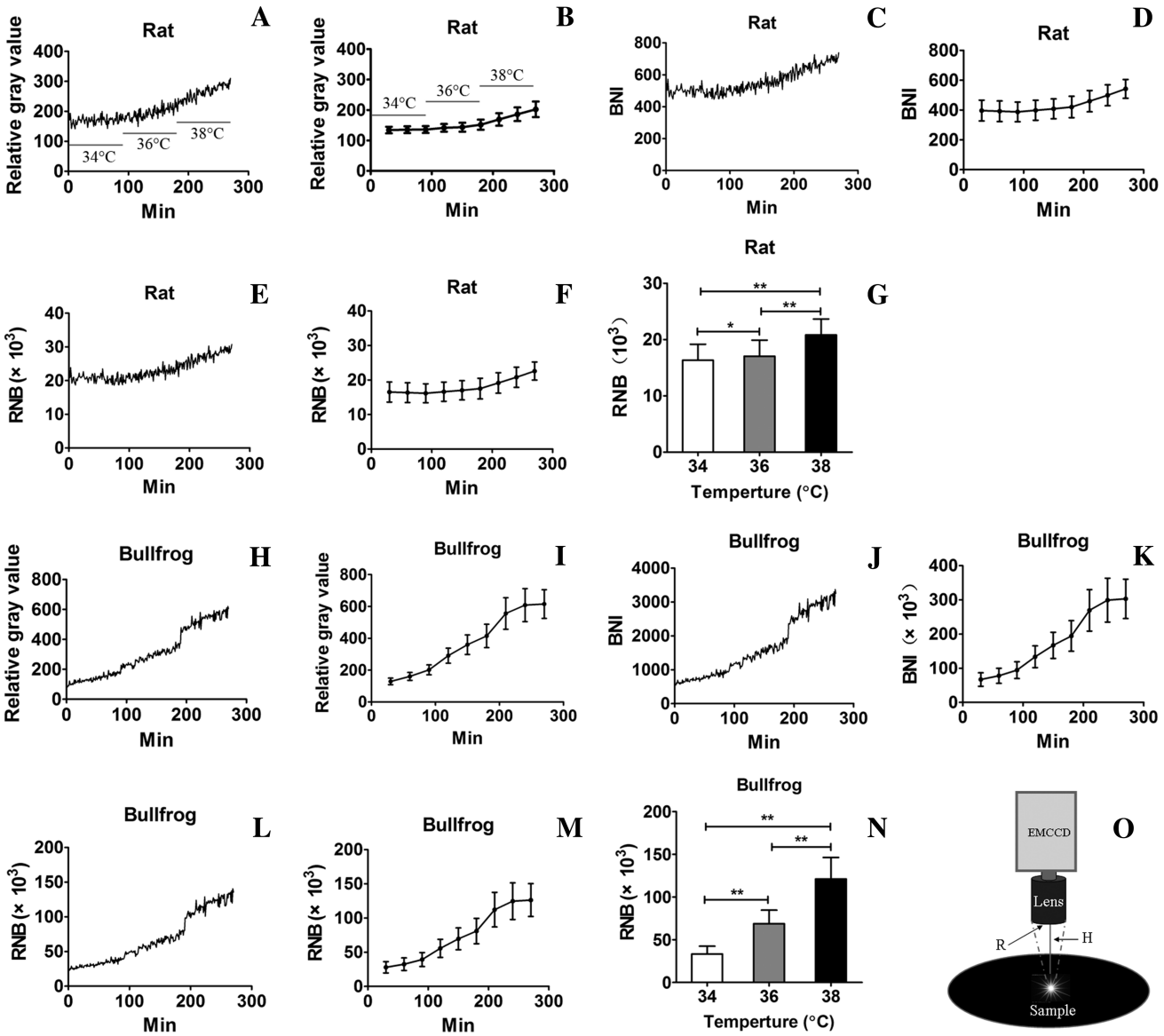


**Fig. 2** Temperature-dependent biophotonic activity in rat and bullfrog retinas. **A–G** Dynamic changes in biophotonic activity in a representative rat retina at 34, 36, and 38 °C shown as relative *gray* value (RGV) (**A**), biophoton number image (BNI) (**C**), and real number of biophotons (RNB) (**E**), as well as the sum of the time course of the average change of RGV (**B**), BNI (**D**), and RNB (**F**) ($n = 5$). **H–N** Similar patterns in bullfrog retina ($n = 6$). **G**, **N** Significant temperature-dependent increases in biophotonic activity in rat and bullfrog retinas from comparison of average change of RNB from 90 continuously-processed biophoton images at 34, 36, and 38 °C. **O** Schematic showing the method of estimation of RNBs in the whole retina based on BNIs, considering the sample as a point light source. **H** Distance between sample and lens (7.0 cm); R, radius of lens (2.5 cm); EMCCD, electron-multiplying CCD camera; the detection quantum efficiency of the EMCCD was 75%.

The sum of the time course of the average change of RGV (B, I), BNI (D, K), and RNB (F, M) was calculated from 30 continuously-processed original gray and biophoton images. Time-course imaging at 1-min intervals are shown in A, C, E, H, J, and L. The duration at each temperature indicated in A and B is identical in C–F and H–M. A two-tailed paired t-test was used to compare the effects of temperature at different time points. Data show the mean ± SEM. $n =$ the number of retinas. $^{*}P < 0.05$, $^{**}P < 0.01$.

## Evaluation of the Intensity of Biophotonic Activity

We evaluated the real number of biophotons (RNBs, Fig. 2E, F, I, L, M) emitted from the whole retina based on the BNIs (Fig. 2C, D, J, K) and a factor of detection

efficiency termed "f". Considering the sample as a point light source, the estimated RNBs of the whole retina based on BNIs can be obtained using RNB $\approx$ BNI/f, where f can be described as $f = E \times \pi R^2/4\pi H^2 = E \times 1/4 \times (R/H)^2 = 0.75 \times 0.25 \times (2.5/7.0)^2 \approx 0.024$; where E is the detection quantum efficiency of the electron-multiplying charge-coupled device (EMCCD) (75%), H is the distance between sample and lens (7.0 cm), and R is the radius of the lens (2.5 cm) (Fig. 2O). The mean RNBs in rat retina at 34, 36, and 38 °C were 41294, 43128, and 52762 photons/cm$^2$/min, respectively, and 38,895, 81,217, and 143,183 photons/cm$^2$/min, in bullfrog retina (Table 1). We calculated the approximate strength of biophoton emission for each photoreceptor (regardless of rod or cone), assuming that virtually all of the detected biophotons originated from the photoreceptors rather than other retinal cells since it is known that neural cells emit few biophotons *in vitro* without additional treatment such as the application of glutamate, an excitatory neurotransmitter [19]. According to previous reports, the rat retina contains about 30 million photoreceptors (mean packing density $37.4 \times 10^6$/cm$^2$) [21]; the *Bufo marinus* (similar to the bullfrog) retina contains about 3.1 million (mean packing density $2.2 \times 10^6$/cm$^2$) [22]. Therefore, we calculated the number of biophotons emitted from each photoreceptor at 34, 36, and 38 °C to be 1.10, 1.15, and $1.41 \times 10^{-3}$ photons/min, respectively, in the rat retina and 17.68, 36.92, and $65.08 \times 10^{-3}$ photons/min in the bullfrog retina (Table 1). We subsequently analyzed the influence of temperature change on biophotonic activity, and found that an increase in temperature from 34 to 38 °C was accompanied by a significant increase in the number of biophotonic emissions in both rat and bullfrog retinas (Fig. 2G, N).

## Effects of $Ca^{2+}$ and Phosphodiesterase

Previous studies have demonstrated that the continuous component of rod dark noise is caused by continuous fluctuations in the cytoplasmic concentrations of both cGMP and $Ca^{2+}$. Such oscillations arise from the activity of both guanylate cyclase, the enzyme that synthesizes cGMP, and PDE, the enzyme that hydrolyzes it [23]. Recently, it was reported that dark events are essentially eliminated in the absence of external $Ca^{2+}$ [24], so we investigated the influence of $Ca^{2+}$ and PDE 6 on biophotonic activity. Removing intracellular and extracellular $Ca^{2+}$ together (Fig. 3A, B), or applying the PDE6 inhibitor Zaprinast (Fig. 3C, D) almost completely blocked the temperature-dependent increase in biophotonic activity in the rat retina.

We used the whole retina rather than a piece of the outer segment to detect the biophotonic activity. So it could be argued that the detected biophotonic activity originated from either the photoreceptor cells or other cell types such as bipolar cells and ganglion cells. However, recent work demonstrating a negligible level of biophotonic activity in mouse brain slices suggests that in the absence of glutamate treatment, neural cells emit very few biophotons during *in vitro* perfusion [19]. In addition, PDE6 is only expressed in retinal photoreceptors [25] and application of

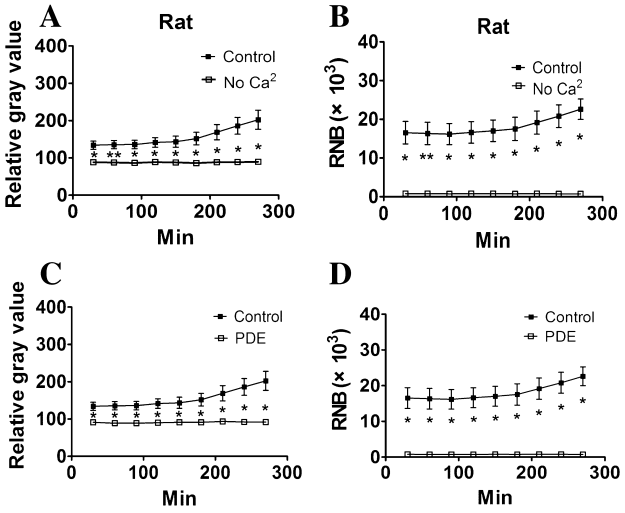


**Fig. 3** Effects of $Ca^{2+}$ and PDE on biophotonic activity in rat retina. **A–D** Removing intra- and extracellular $Ca^{2+}$ together (**A** and **B**, 10 μmol/L BAPTA-AM + 0.5 mmol/L EGTA, $n = 5$) or introducing a PDE inhibitor (**C** and **D**, 100 nmol/L Zaprinast, $n = 6$) almost completely blocked biophotonic activity in the retina at 34, 36, and 38 °C. The duration at each temperature was 0–90 min at 34 °C, 91–180 min at 36 °C, and 181–270 min at 38 °C. The control data ($n = 5$) from Fig. 2**B** and **F** were used for statistical comparison. Data show the mean ± SEM. $n$ = number of retinas. $^*P < 0.05$; $^{**}P < 0.01$.

**Table 1** The evaluated number of biophoton emissions per min in retinal photoreceptors in different temperatures (mean ± SEM).

| | 34 °C | 36 °C | 38 °C |
|---|---|---|---|
| Rat ($n = 5$) | | | |
| cm$^2$/min ($10^3$) | 41.29 ± 6.83 | 43.13 ± 6.91 | 52.76 ± 6.84 |
| Per cell/min ($10^{-3}$) | 1.10 ± 0.18 | 1.15 ± 0.18 | 1.41 ± 0.18 |
| Bullfrog ($n = 6$) | | | |
| cm$^2$/min ($10^3$) | 39.90 ± 10.59 | 81.22 ± 18.31 | 143.20 ± 28.85 |
| Per cell/min ($10^{-3}$) | 17.68 ± 4.81 | 36.92 ± 8.32 | 65.08 ± 13.11 |

the PDE6 inhibitor Zaprinast almost completely blocked the temperature-dependent increase in biophotonic activity in the rat retina. Therefore, we can conclude that the recorded biophotonic activity originated almost entirely from the photoreceptors. In the present study, we imaged retinal biophoton emission by slowly raising the temperature, but not by repeatedly reducing and elevating the temperature, which has been used to analyze retinal dark noise with electrophysiological recordings in the short-term (<2 min) and at relatively low temperatures (15–30 °C) [1, 26]. This was because repeated switching between 34 and 38 °C for a prolonged period would cause abnormal stress in the retina that may not only have resulted in additional biophoton emission, but also disturbed the normal physiological condition of the retina.

Although the exact biological importance of the biophotonic activity of retinal photoreceptors is not clear, our findings provide a novel and reasonable explanation for the origin and mechanisms of discrete dark noise in photoreceptors. Because biophotons are naturally similar to visual light [14], we propose that the photon-like component of the discrete dark noise may not be directly due to the thermal activation of rhodopsin, as has been emphasized in previous studies [3–8], but rather to the indirect thermal induction of biophotonic activity that then activates the retinal chromophore of rhodopsin. Such a mechanism of action suggests that a thermal activation energy barrier does not exist or is not necessary for biophotonic isomerization of the PSB11 chromophore. The observed temperature-dependent increase in biophotonic activity may be associated with a change in metabolic activity, which has been proposed as the origin of background biophotons [18]. The existence of such background biophotonic activity may provide additional evidence to explain the long-wavelength sensitivity changes with temperature in retinal pigment cells [27]; isomerization of the PSB11 chromophore may occur *via* multi-photon excitation between background biophotons and external natural light so that their energy is pooled [28]. This may explain the well-documented finding that pigments with longer peak-absorption wavelengths are noisier and thus less suitable for dim-light detection. Therefore, pigments with longer peak-absorption wavelengths are easily activated by biophotons and result in more noise, but the noise would have a lower peak amplitude and a faster time course. This may also explain why noise rates are higher in cone pigments than rod pigments for the rhodopsins of a given peak-absorption wavelength, since the former have a higher aerobic metabolic rate than the latter [29], and the generation of biophotons is associated with lipid oxidation, mitochondrial respiration, and other metabolic activity [30, 31].

Previous studies have shown that the continuous component of rod dark noise is caused by continuous fluctuations in the cytoplasmic concentrations of both cGMP and $Ca^{2+}$. Such oscillations arise from the activity of both guanylate cyclase and PDE [23]. Recently, it was found that dark events are essentially eliminated in the absence of external $Ca^{2+}$ in *Drosophila* photoreceptors [24]. The complete suppression of temperature-dependent biophotonic activity by removing both extracellular and intracellular $Ca^{2+}$ or *via* application of a PDE6 inhibitor suggests the involvement of both $Ca^{2+}$ and PDE in the production of photoreceptor biophotons though the detailed mechanisms are not clear.

Although our findings provide a novel explanation for the origin of retinal dark noise, key questions must be answered to establish a solid relationship between biophotons and retinal dark noise. For example, it is necessary to establish the rate of discrete thermal activation in photoreceptors and its correlation with the biophoton emission at each temperature by combining electrophysiological methods such as patch-clamping and UBIS. This could also provide an explanation for the different roles of porphyropsin and rhodopsin rods [32, 33]. However, it is clear that the combination of such techniques presents technical and practical difficulties that need to be solved.

**Acknowledgments** This work was supported by the National Natural Science Foundation of China (31070961), the Sci-Tech Support Plan of Hubei Province, China (2014BEC086), and the Research Team Fund of South Central University for Nationalities, China (XTZ15014). We also thank to Fangyang Xiao for secretarial help.

## References

1. Baylor DA, Matthews G, Yau KW. Two components of electrical dark noise in toad retinal rod outer segments. The Journal of Physiology 1980, 309: 591–621.
2. Rieke F, Baylor DA. Molecular origin of continuous dark noise in rod photoreceptors. Biophysical Journal 1996, 71: 2553–2572.
3. Barlow RB, Birge RR, Kaplan E, Tallent JR. On the molecular origin of photoreceptor noise. Nature 1993, 366: 64–66.
4. Liu J, Liu MY, Nguyen JB, Bhagat A, Mooney V, Yan EC. Thermal decay of rhodopsin: role of hydrogen bonds in thermal isomerization of 11-cis retinal in the binding site and hydrolysis of protonated Schiff base. Journal of the American Chemical Society 2009, 131: 8750–8751.
5. Liu J, Liu MY, Nguyen JB, Bhagat A, Mooney V, Yan EC. Thermal properties of rhodopsin: insight into the molecular mechanism of dim-light vision. The Journal of Biological Chemistry 2011, 286: 27622–27629.
6. Lorenz-Fonfria VA, Furutani Y, Ota T, Ido K, Kandori H. Protein fluctuations as the possible origin of the thermal activation of rod photoreceptors in the dark. Journal of the American Chemical Society 2010, 132: 5693–5703.
7. Kukura P, McCamant DW, Yoon S, Wandschneider DB, Mathies RA. Structural observation of the primary isomerization in vision with femtosecond-stimulated Raman. Science 2005, 310: 1006–1009.
8. Gozem S, Schapiro I, Ferre N, Olivucci M. The molecular mechanism of thermal noise in rod photoreceptors. Science 2012, 337: 1225–1228.

9. Ala-Laurila P, Donner K, Koskelainen A. Thermal activation and photoactivation of visual pigments. Biophysical Journal 2004, 86: 3653–3662.
10. Luo DG, Yue WW, Ala-Laurila P, Yau KW. Activation of visual pigments by light and heat. Science 2011, 332: 1307–1312.
11. Khrenova MG, Bochenkova AV, Nemukhin AV. Modeling reaction routes from rhodopsin to bathorhodopsin. Proteins 2010, 78: 614–622.
12. Barlow HB. Purkinje shift and retinal noise. Nature 1957, 179: 255–256.
13. Ala-Laurila P, Pahlberg J, Koskelainen A, Donner K. On the relation between the photoactivation energy and the absorbance spectrum of visual pigments. Vision Research 2004, 44: 2153–2158.
14. Cohen S, Popp FA. Biophoton emission of human body. Indian Journal of Experimental Biology 2003, 41: 440–445.
15. Albrecht-Buehler G. Rudimentary form of cellular "vision". Proceedings of the National Academy of Sciences of the United States of America 1992, 89: 8288–8292.
16. Farhadi A, Forsyth C, Banan A, Shaikh M, Engen P, Fields JZ, *et al.* Evidence for non-chemical, non-electrical intercellular signaling in intestinal epithelial cells. Bioelectrochemistry 2007, 71: 142–148.
17. Fels D. Cellular communication through light. PloS One 2009, 4: e5086.
18. Sun Y, Wang C, Dai J. Biophotons as neural communication signals demonstrated by in situ biophoton autography. Photochemical and Photobiological Sciences 2010, 9: 315–322.
19. Tang R, Dai J. Spatiotemporal imaging of glutamate-induced biophotonic activities and transmission in neural circuits. PloS One 2014, 9: e85643.
20. Tang R, Dai J. Biophoton signal transmission and processing in the brain. Journal of Photochemistry and Photobiology B, Biology 2014, 139: 71–75.
21. Mayhew TM, Astle D. Photoreceptor number and outer segment disk membrane surface area in the retina of the rat: stereological data for whole organ and average photoreceptor cell. Journal of Neurocytology 1997, 26: 53–61.
22. Zhang YD, Straznicky C. The morphology and distribution of photoreceptors in the retina of *Bufo marinus*. Anatomy and Embryology 1991, 183: 97–104.
23. Holcman D, Korenbrot JI. The limit of photoreceptor sensitivity: molecular mechanisms of dark noise in retinal cones. The Journal of General Physiology 2005, 125: 641–660.
24. Katz B, Minke B. Phospholipase C-mediated suppression of dark noise enables single-photon detection in Drosophila photoreceptors. The Journal of Neuroscience 2012, 32: 2722–2733.
25. Yamazaki A, Moskvin O, Yamazaki RK. Phosphorylation by cyclin-dependent protein kinase 5 of the regulatory subunit (Pgamma) of retinal cgmp phosphodiesterase (PDE6): its implications in phototransduction. Advances in Experimental Medicine and Biology 2002, 514: 131–153.
26. Baylor DA, Matthews G, Yau KW. Temperature effects on the membrane current of retinal rods of the toad. The Journal of Physiology 1983, 337: 723–734.
27. Ala-Laurila P, Albert RJ, Saarinen P, Koskelainen A, Donner K. The thermal contribution to photoactivation in A2 visual pigments studied by temperature effects on spectral properties. Visual Neuroscience 2003, 20: 411–419.
28. Benninger RK, Hao M, Piston DW. Multi-photon excitation imaging of dynamic processes in living cells and tissues. Reviews of Physiology, Biochemistry and Pharmacology 2008, 160: 71–92.
29. Perkins GA, Ellisman MH, Fox DA. Three-dimensional analysis of mouse rod and cone mitochondrial cristae architecture: bioenergetic and functional implications. Molecular Vision 2003, 9: 60–73.
30. Zhuravlev AI, Tsvylev OP, Zubkova SM. [Spontaneous endogenous ultraweak luminescence of rat liver mitochondria in conditions of normal metabolism]. Biofizika 1973, 18: 1037–1040.
31. Dotta BT, Buckner CA, Cameron D, Lafrenie RF, Persinger MA. Biophoton emissions from cell cultures: biochemical evidence for the plasma membrane as the primary source. General Physiology and Biophysics 2011, 30: 301–309.
32. Donner K, Firsov ML, Govardovskii VI. The frequency of isomerization-like 'dark' events in rhodopsin and porphyropsin rods of the bull-frog retina. The Journal of Physiology 1990, 428: 673–692.
33. Ala-Laurila P, Donner K, Crouch RK, Cornwall MC. Chromophore switch from 11-cis-dehydroretinal (A2) to 11-cis-retinal (A1) decreases dark noise in salamander red rods. The Journal of Physiology 2007, 585: 57–74.